Available online at www.sciencedirect.com
ScienceDirect
Polymer 48 (2007) 4174–4183
polymer
www.elsevier.com/locate/polymer

Thermal expansion behavior of composites based on axisymmetric ellipsoidal particles

K.Y. Lee [a], K.H. Kim [a], S.K. Jeoung [b], S.I. Ju [a], J.H. Shim [c], N.H. Kim [d], S.G. Lee [e], S.M. Lee [f], J.K. Lee [f], D.R. Paul [g,*]

[a] Department of Polymer and Biomaterial Engineering, Chungnam National University, Daejeon, South Korea
[b] Korea Automotive Technology Institute, Chonan, South Korea
[c] LG Chem., Ltd. Daejeon, South Korea
[d] Hanwha L & C Corporation, Cheongwon, South Korea
[e] Department of Advanced Organic Materials and Textile System Engineering, Chungnam National University, Daejeon, South Korea
[f] Honam Petrochemical Corporation, Daedeok Research Institute PP1 Research Group, Daejeon, South Korea
[g] Department of Chemical Engineering, Texas Materials Institute, University of Texas at Austin, Austin, TX 78712, USA

Received 29 December 2006; received in revised form 15 May 2007; accepted 16 May 2007
Available online 21 May 2007

Abstract

A new model for calculating the coefficients of thermal expansion, CTE, in all three coordinate directions is developed for composites containing aligned, axisymmetric elliptical particles, i.e., characterized by a single aspect ratio, that in the limit approximate the shapes of spheres, fibers and discs. This model is based on Elshelby's method but employs a somewhat different formulation than used in prior papers; a main advantage of the current approach is that it can be readily extended to composites based on ellipsoidal particles with no axes of symmetry, i.e., all three major axes are different, as recently demonstrated for modulus. CTE predictions for the simple case of axisymmetric particles are illustrated by calculations for glass particles in the shape of spheres, fibers and discs in an epoxy resin and are compared to those from the popular Chow theory. For spherical-shaped particles, the CTEs in all directions are the same and decrease modestly as the volume fraction of filler particles increases. As the particle aspect ratio increases from unity, the thermal expansion becomes anisotropic. The coefficient of longitudinal linear thermal expansion always decreases with increasing aspect ratio and filler loading due to the mechanical constraint of the filler. For aligned axisymmetric particles, the coefficients of linear thermal expansion are always the same in two directions. The values in the transverse direction may be higher or lower than that of the matrix depending on the values of aspect ratio and filler loading; these regions are mapped out for this particular set of matrix and filler properties. The two-dimensional constraints on matrix expansion caused by discs versus the one-dimensional effects of fibers cause quantitative differences in behavior for the two shapes.

Keywords: Composites; Ellipsoidal particles; Thermal expansion

1. Introduction

Theoretical and empirical relations between the structure of two-phase materials and their properties have been studied for decades [1–32]. The mechanical and thermal properties of composites based on a polymer matrix with dispersed inclusions have been a particular interest. It is generally expected that the mechanical and thermal properties of composites are dependent on the shape, the orientation, and properties of the included particles plus their adhesion to the matrix. The basic theories needed to model composites containing inclusions characterized by a single aspect ratio, such as spheres ($\rho_\alpha = 1$, $a_1 = a_2 = a_3$), fibers ($a_1 > a_2 = a_3$), and discs ($a_1 = a_2 > a_3$), are well known, where a_1 is the dimension of the

* Corresponding author. Tel.: +1 512 471 5392; fax: +1 512 471 0542.
E-mail address: drp@che.utexas.edu (D.R. Paul).

0032-3861/$ - see front matter © 2007 Elsevier Ltd. All rights reserved.
doi:10.1016/j.polymer.2007.05.036

inclusion in the x_1 direction and the others can be readily understood (see Fig. 1). Mura [6] showed how to use these theories to formulate explicit expressions for the components of the tensors of ellipsoidal inclusions.

Much of the prior literature has focused on fiber reinforcement, but with the advent of nanocomposites, there is a growing interest in fillers with other shapes like platelets that may be irregular in dimensions. In this paper, we describe a theoretical approach for predicting the coefficient of thermal expansion, CTE, behavior of composites containing spherical, fiber-like and two-dimensional disc-like ellipsoidal inclusions characterized by a single aspect ratio, $\rho_\alpha = a_1/a_3$. The particles are assumed to be uniformly distributed and unidirectionally aligned within the composite as well as being well bonded to the matrix. The properties of the matrix and the filler are assumed to be isotropic and known. The analysis used here follows the procedure developed earlier for the elastic moduli of composites [5,9] and differs from that of Takao and Taya [13] in certain details.

An advantage of the current approach is that it can be readily extended to composites based on ellipsoidal particles where all three major axes are at different t, i.e., $a_1 \neq a_2 \neq a_3$, such that two aspect ratios are needed to characterize them as was shown in a recent paper on the modulus of such composites [9]. In a subsequent paper, we will present the analogous treatment of CTE behavior which is of particular interest for polymer nanocomposites used in automotive applications.

2. Background

The development of the self-consistent theory that follows makes use of Eshelby's equivalent transformation strain [1] of inclusions, Hill's limitation of the upper and the lower bounds for the effective mechanical properties of composites [2], Hill's idea of stress- and strain-concentration tensors and Mori–Tanaka's average stress [3].

Many different approaches ranging from ones based on empirical data for polymer composites to sophisticated analytical or numerical analyses based on applied mechanics have been reported in the literature. Schapery [14] and Wakashima et al. [15] proposed a way to determine the effective CTE of isotropic and anisotropic composite materials consisting of isotropic phases by employing principles of thermo-elasticity based on energy considerations. Chow [10–12] developed a theory for the effects of particle shape on the thermal and mechanical properties of filled polymers. Takao and Taya [13] also proposed a theoretical formulation for CTE using the concepts of eigenstrain and transformation strain. Mean-field of Eshelby-based homogenization techniques for thermo-elastic composites was published by Pierard et al. [26]. For two- and multi-phase composites, direct homogenization schemes which lead to a non-symmetric overall stiffness tensor were introduced. Li [27] studied non-symmetric effective moduli with an effective-medium-field micromechanics approximation using normalized concentration factors by the Mori–Tanaka and self-consistent approaches. The effects of misaligned particles were described by Doghri and Tinel [28] using micromechanics with mean-field homogenization methods for volume and orientation averaging.

Direct predictions of CTE behavior using a finite-element based numerical approach for short-fiber reinforced composites were reported recently by Lusti et al. [29]. Dray et al. [30] compared the thermo-elastic properties of injection molded short-fiber composites predictions by several closure approximations. Recently, Hbaieb et al. [31] modeled the stiffness of polymer/clay nanocomposites via two- and three-dimensional finite-element methods using the commercial software ABACUS.

Ellis and D'Angelo [21] studied the thermal and mechanical properties of a polypropylene nanocomposite, containing approximately 4 wt% of an organophilic montmorillonite clay and 20% talc-filled PP. Research on the CTE of carbon nanotube polymer composites was also recently conducted by Wei et al. [22]. Lee et al. [23,24] reported experimental data for nanocomposites based on blends of polypropylene, elastomer and an organoclay. The thermal expansion behavior was interpreted in terms of the morphology of both the elastomer domains and the filler particles. Comparisons among several analyses for predicting the CTE of composites containing unidirectional graphite fibers in the longitudinal and transverse directions with experimental data were made by Bowles and Tompkins [25].

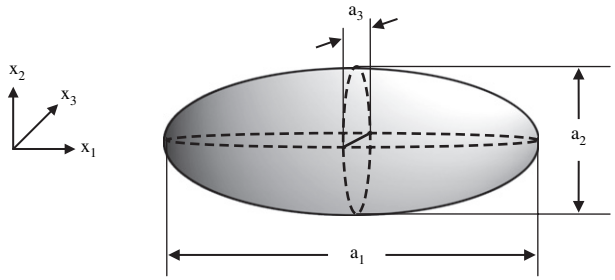

Fig. 1. Schematic representation of ellipsoidal inclusions, or filler particles, characterized by a single aspect ratio $\rho_\alpha = a_1/a_3$. The case where $a_1 = a_2 = a_3$, corresponds to a sphere while fibers are approximated by $a_1 > a_2 = a_3$, and discs by $a_1 = a_2 > a_3$.

3. Model development

3.1. Basic theory

As the temperature changes in a two-phase composite, an internal strain develops that can be expressed as follows:

$$\overline{e}_{ij} = (\alpha_f - \alpha_m)\Delta T \delta_{ij} \quad (1)$$

where α_m and α_f are the linear CTE of the matrix and the inclusion, respectively; $\overline{e}_{ij}$ is the internal strain, eigenstrain or thermal strain defined by Mura [6] due to the difference between α_f and α_m; ΔT is the temperature change; and δ_{ij} is the

Kronecker delta. The internal strain can also be expressed in terms of the linear CTE for the composite, α_{ij} as follows:

$$\overline{e}_{ij} = \alpha_{ij}\Delta T\delta_{ij} \tag{2}$$

For the ideal condition of free external stress and uniform surface traction on the boundaries of the composite, the internal strains due to the thermal expansion and the external strain can be analyzed by the average stress [3]. In composite materials, the external strain, $\overline{\varepsilon}$, is related to the internal strain $\overline{e}$ due to the thermal expansion and the applied volume-average stress, $\overline{\sigma}$, via the elastic moduli tensor of the composite, $\overline{C}$, which contains contributions from the elastic modulus tensor for the matrix and that of the perfectly aligned ellipsoidal inclusions. In the thermal expansion problem, the external average stress can be expressed by [6]

$$\overline{\sigma} = \overline{C}(\overline{\varepsilon} - \overline{e}) \tag{3}$$

As the temperature changes in the absence of an external load, the external stress will be zero, and the expansional internal strain can be expressed by the external strain, $\overline{\varepsilon}$, as follows:

$$\overline{\varepsilon} = \overline{e} \tag{4}$$

The average strain over an adequate system volume $\overline{\varepsilon}$ is not equal to the homogeneous strain ε^{m} due to the presence of the inclusions. This problem has to do with the perturbation strains of the matrix $\tilde{\varepsilon}^{\mathrm{m}}$ and filler $\tilde{\varepsilon}^{\mathrm{f}}$, which are the differences between the local strain and the average strain, and correspond to the average perturbed stresses for the matrix, $\tilde{\sigma}^{\mathrm{m}}$, and for the filler, $\tilde{\sigma}^{\mathrm{f}}$, respectively. These are related as follows [5]

$$\overline{\varepsilon} = \varepsilon^{\mathrm{m}} + \tilde{\varepsilon}^{\mathrm{m}} + \tilde{\varepsilon}^{\mathrm{f}}, \tag{5}$$

In order to predict CTE behavior, we simply follow the derivation by Lee and Paul [9] based on Eshelby's equivalent principle [1], using the equivalent transformation strain of the inclusion, ε^{t}, for the ellipsoidal shaped inclusions without external volume-average stress ($\overline{\sigma} = 0$). The stress equivalence in the inclusion may be expressed by [5]

$$\tilde{\sigma}^{\mathrm{m}} + \tilde{\sigma}^{\mathrm{f}} = C^{\mathrm{f}}\left(\varepsilon^{\mathrm{m}} + \tilde{\varepsilon}^{\mathrm{m}} + \tilde{\varepsilon}^{\mathrm{f}}\right) = C^{\mathrm{m}}\left(\varepsilon^{\mathrm{m}} + \tilde{\varepsilon}^{\mathrm{m}} + \tilde{\varepsilon}^{\mathrm{f}} - \varepsilon^{\mathrm{t}}\right) \tag{6}$$

The relationship between transformation strain and thermal strain due to the mismatch of α_{m} and α_{f} was defined differently by Takao and Taya [13]. The average strain of the composite over the matrix and its inclusions, $\overline{\varepsilon}$, is related to the volume fraction of inclusions ϕ, as follows [9]

$$\overline{\varepsilon} = \varepsilon^{\mathrm{m}} + \phi\varepsilon^{t} \tag{7}$$

As temperature changes, the pure homogeneous matrix, free of any external stresses, induces the same amount of internal strains in the three directions as an isotropic matrix due to the thermal expansion; i.e., $\varepsilon^{\mathrm{m}} = \varepsilon^{\mathrm{m}}_{11} = \varepsilon^{\mathrm{m}}_{22} = \varepsilon^{\mathrm{m}}_{33}$ and $(\alpha_{\mathrm{m}})_{11} = (\alpha_{\mathrm{m}})_{22} = (\alpha_{\mathrm{m}})_{33} = \alpha_{\mathrm{m}}$. Therefore, we can get

$$\frac{\overline{\varepsilon}}{\varepsilon^{\mathrm{m}}} = 1 + \phi\frac{\varepsilon^{\mathrm{t}}}{\varepsilon^{\mathrm{m}}} = \frac{\alpha_{ij}}{\alpha_{\mathrm{m}}} \tag{8}$$

and

$$\frac{\alpha_{ij}}{\alpha_{\mathrm{m}}} = 1 + \phi\frac{\varepsilon^{\mathrm{t}}_{ij}}{\alpha_{\mathrm{m}}\Delta T\delta_{ij}} = 1 + \phi A^{\mathrm{t}}_{ij} \tag{9}$$

where

$$A^{\mathrm{t}}_{ij} = \frac{\varepsilon^{\mathrm{t}}_{ij}}{\alpha_{\mathrm{m}}\Delta T\delta_{ij}} \tag{10}$$

Here, A^{t}_{ij} corresponds to the transformation strain tensor, ε^{t}, given by Eshelby's equivalent principle. The ratio of the equivalent transformation strain to the coefficient of the linear thermal expansion matrix, A^{t}_{ij}, can be determined from the second part of Eq. (6). Next, the linear CTE of the composite material, α_{ij}, can then be calculated from the linear CTE of the pure matrix, α_{m}, and the volume fraction of filler from Eq. (9).

From Eq. (8), it can be seen that α_{ij} is linearly proportional to the average strain of the composite, $\overline{\varepsilon}$, without any external stress, that results from temperature changes. On the contrary, the longitudinal Young's modulus, E_{11}, with external strain is exactly inversely proportional to the average strain, from Eq. (32) in Lee and Paul [9]. The relationship between α_{11} and E_{11} is shown to be inverse in the current model.

Chow [12] reviewed the effect of particle shape on the mechanical and thermal properties of filled polymers, using different notations and definitions of the perturbed strain of inclusion and gave the following expressions:

$$\frac{E_{11}}{E_{\mathrm{m}}} = 1 + \frac{(k_{\mathrm{f}}/k_{\mathrm{m}} - 1)G_3 + 2(\mu_{\mathrm{f}}/\mu_{\mathrm{m}} - 1)K_3}{2K_3G_1 + G_3K_1}\phi \tag{11}$$

$$\frac{\alpha_{11}}{\alpha_{\mathrm{m}}} = 1 + \frac{k_{\mathrm{f}}/k_{\mathrm{m}}(\gamma_{\mathrm{f}} - \gamma_{\mathrm{m}})G_3}{2K_3G_1 + G_3K_1}\frac{\phi}{\alpha_{\mathrm{m}}} \tag{12}$$

$$\text{where} \quad K_i = 1 + (k_{\mathrm{f}}/k_{\mathrm{m}} - 1)(1 - \phi)\alpha_i \tag{13}$$

$$\text{and} \quad G_i = 1 + (\mu_{\mathrm{f}}/\mu_{\mathrm{m}} - 1)(1 - \phi)\beta_i \quad (i = 1,3) \tag{14}$$

where the parameters α_i and β_i are functions of the aspect ratio ρ_α and the Poisson's ratio of the matrix, see Appendix of Ref. [10]. According to Chow, the CTE of composites, α_{11}, in Eq. (12) has the same denominator as the expression for the longitudinal Young's modulus, E_{11}, in Eq. (11). In the current model, the connection between α_{11} and E_{11} is not so simple as in the Chow model.

3.2. Calculation of A^{t}_{ij}

The simple limiting cases of two-dimensional ellipsoidal inclusions are illustrated in Fig. 1. The components of Eshelby's transformation tensor, S_{ijkl}, can be written as shown in Appendix. They are dependent upon the geometry of the inclusions and the Poisson's ratio of the matrix.

By use of Eqs. (2), (6) and (9), the ratio of the equivalent transformation strain, A^{t}_{ij}, can be expressed by

$$\left(C^{f}_{ijkl} - C^{m}_{ijkl}\right)\left[1 + (1-\phi)S_{klmn}A^{t}_{ij} + \phi A^{t}_{ij}\right] + C^{m}_{ijkl}A^{t}_{ij} = 0 \quad (15)$$

Eq. (15) allows us to calculate A^{t}_{ij} in terms of known parameters, such as ϕ, C^{m}_{ijkl}, C^{f}_{ijkl} and S_{klmn}, and can be rearranged into linear simultaneous equations as follows

$$B_1A^{t}_{11} + B_2A^{t}_{22} + B_2A^{t}_{33} = D_4 \quad (16)$$

$$B_3A^{t}_{11} + B_4A^{t}_{22} + B_5A^{t}_{33} = D_4 \quad (17)$$

$$B_3A^{t}_{11} + B_5A^{t}_{22} + B_4A^{t}_{33} = D_4 \quad (18)$$

where

$$\begin{aligned}
B_1 &= \phi D_1 + D_2 + (1-\phi)(D_1S_{1111} + 2S_{2211})\\
B_2 &= \phi + D_3 + (1-\phi)(D_1S_{1122} + S_{2222} + S_{2233})\\
B_3 &= \phi + D_3 + (1-\phi)[S_{1111} + (1+D_1)S_{2211}]\\
B_4 &= \phi D_1 + D_2 + (1-\phi)(S_{1122} + D_1S_{2222} + S_{2233})\\
B_5 &= \phi + D_3 + (1-\phi)(S_{1122} + S_{2222} + D_1S_{2233})
\end{aligned}$$

and

$$\begin{aligned}
D_1 &= 1 + 2(\mu_f - \mu_m)/(\lambda_f - \lambda_m)\\
D_2 &= (\lambda_f + 2\mu_m)/(\lambda_f - \lambda_m)\\
D_3 &= \lambda_m/(\lambda_f - \lambda_m)\\
D_4 &= -2(\mu_f - \mu_m)/(\lambda_f - \lambda_m) - 3
\end{aligned}$$

where λ_m, μ_m and λ_f, μ_f are the *Lame'* constants of the matrix and inclusions, respectively.

From Eqs. (16)–(18), the ratio of the equivalent transformation strain, A^{t}_{11} and A^{t}_{33} can be calculated as follows

$$A^{t}_{11} = \frac{D_4(2B_2 - B_4 - B_5)}{(2B_2B_3 - B_1B_4 - B_1B_5)}, \quad (19)$$

$$\text{and } A^{t}_{33} = \frac{D_4(B_3 - B_1)}{(2B_2B_3 - B_1B_4 - B_1B_5)} \quad (20)$$

3.3. Calculation of the coefficients of thermal expansion

Composite materials, in general, have different CTEs in each of the three coordinate directions; however, when the inclusions are characterized by a single aspect ratio and are aligned along the axis directions, two of these coefficients are equal. The longitudinal CTE, α_{11}, can be determined from A^{t}_{11}, of Eq. (19) and the effect of volume fraction of filler from Eq. (9)

$$\frac{\alpha_{11}}{\alpha_m} = 1 + \phi\frac{D_4(2B_2 - B_4 - B_5)}{(2B_2B_3 - B_1B_4 - B_1B_5)} \quad (21)$$

Similarly, the CTE, α_{33}, for such composites can be determined from A^{t}_{33} of Eq. (20) and the effect of volume fraction of filler using Eq. (9)

$$\frac{\alpha_{33}}{\alpha_m} = 1 + \phi\frac{D_4(B_3 - B_1)}{(2B_2B_3 - B_1B_4 - B_1B_5)} \quad (22)$$

For the fiber-like inclusions, the transverse CTE α_{22} and the bulk CTE γ are expressed by

$$\alpha_{22} = \alpha_{33} \quad (23)$$

$$\gamma = \alpha_{11} + 2\alpha_{33} \quad (24)$$

For disc-like inclusions, the CTE α_{22} and the bulk CTE γ are expressed by

$$\alpha_{22} = \alpha_{11} \quad (25)$$

$$\gamma = 2\alpha_{11} + \alpha_{33} \quad (26)$$

4. Numerical results and discussion

The effects of the aspect ratio and the volume fraction of inclusions on the CTE are illustrated here for composites consisting of glass particles of various shapes in an epoxy resin matrix. The material properties of the epoxy resin and the glass particles taken from the literature [5,32] are listed in Table 1; the properties of the glass determined for fibers are assumed, in the absence of other information, to apply for other shapes.

The predicted CTEs of composites, normalized by that of the matrix, in the longitudinal direction α_{11}/α_m and the transverse direction α_{33}/α_m are shown in Fig. 2 as a function of the aspect ratio ρ_α ($=a_1/a_3$) for given volume fractions of filler ranging from $\phi = 0.1$ to 0.5. The results for disc-like inclusions (or discs) in Fig. 2(a) show similar trends as seen for fiber-like inclusions (or fibers) in Fig. 2(b). For spherical inclusions, the coefficients ($\alpha_{33} = \alpha_{11}$) are simply a function of the concentration of filler and decrease as ϕ increases mainly due to dilution of the matrix, which has a higher thermal expansion, with the filler, which has a lower thermal expansion. The longitudinal CTE ratio to that of the polymer matrix, α_{11}/α_m, monotonically decreases with filler concentration ϕ as the aspect ratio increases from unity; conversely, the transverse CTE ratio, α_{33}/α_m, increases with aspect ratio for all ϕ.

The decrease in α_{11}/α_m with aspect ratio is due to the mechanical constraint the filler provides against the expansion of the matrix in the longitudinal direction. On the contrary, the transverse thermal expansion α_{33}/α_m increases with aspect ratio (for low enough ϕ) since the longitudinal restraint by the inclusions squeezes the polymer matrix outwardly in the

Table 1
Material properties for epoxy resin and glass fibers

	Density (Kg/m^3)	Modulus (GPa)		Linear CTE × 10^6 (K^{-1})		Poisson's ratio		Bulk modulus (GPa)
Epoxy	1200	E_m	2.76	α_m	81	ν_m	0.35	3.06
Glass fiber	2540	E_f	72.4	α_f	5.0	ν_f	0.20	40.2

The material constants were taken from Refs. [5,27].

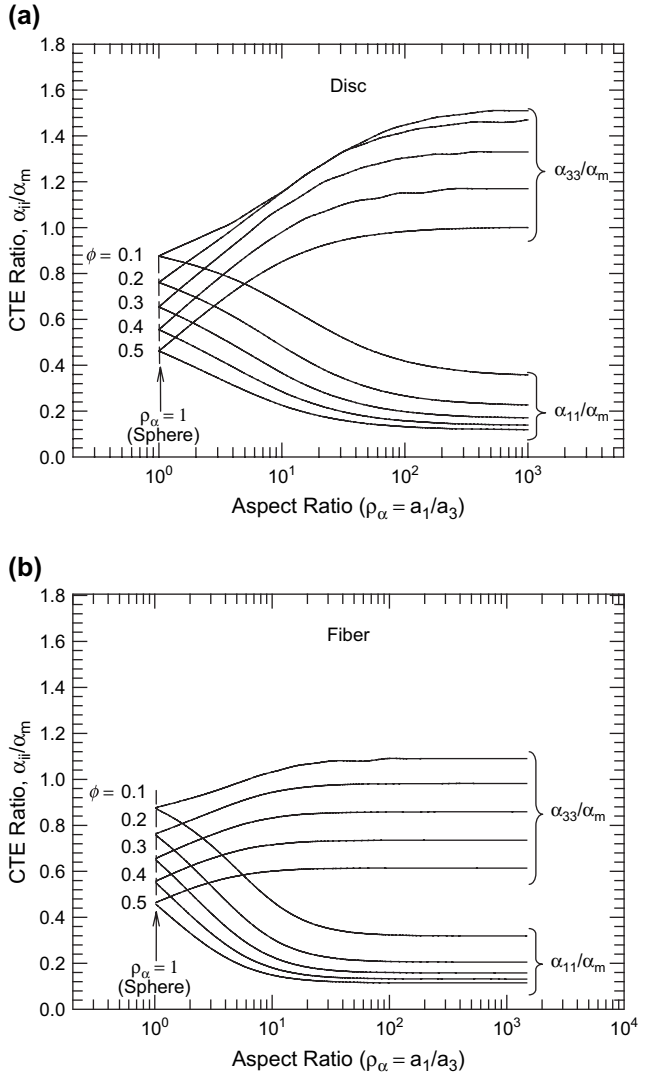

Fig. 2. Normalized coefficients of longitudinal, α_{11}/α_m, and transverse, α_{33}/α_m, thermal expansion for the disc-shaped (a) and fiber-shaped inclusions (b) as a function of aspect ratio, ρ_α, for various filler volume fractions, ϕ. Calculations represent the case where the components have the properties listed in Table 1.

transverse direction. Therefore, the influence of aspect ratio, for a given volume fraction of filler, leads to opposite effects on the longitudinal and transverse CTEs.

The rate of decrease of α_{11}/α_m with aspect ratio, for a given ϕ, is somewhat greater for fibers than for discs. In addition, the rate of initial increase of α_{33}/α_m with aspect ratio for fixed ϕ is less for fibers than discs. The expansion change in the x_2 direction is the same as that in the x_1 direction for discs, i.e., $\alpha_{22}/\alpha_m = \alpha_{11}/\alpha_m$, while for fibers it is the same as in the x_3 direction, $\alpha_{22}/\alpha_m = \alpha_{33}/\alpha_m$. Generally, one is interested in reducing the linear CTE, and the advantages of discs is that they reduce expansion in two directions ($\alpha_{11} = \alpha_{22} < \alpha_{33}$), while fibers only do so in one direction ($\alpha_{11} < \alpha_{22} = \alpha_{33}$).

For discs and fibers, the thermal expansion coefficients in the longitudinal α_{11} and transverse α_{33} directions approach fixed values for each volume fraction, ϕ, as the aspect ratio increases in Fig. 2.

The CTEs of composites, α_{11}/α_m and α_{33}/α_m, predicted by the current model are compared with those from the Chow model in Fig. 3 as a function of the aspect ratio ρ_α ($=a_1/a_3$) for fixed volume fractions of filler $\phi = 0.25$, 0.5 and 0.75. The results for discs predicted by the current model show similar trends as the Chow model in Fig. 3(a), while the difference between the two models is greater for fibers as shown in Fig. 3(b).

In all cases, the CTE in the limit as $\rho_\alpha \to \infty$ (or >100), approach a constant value as expected by a simple rule of mixtures for Young's modulus and thermal expansion, as proposed by Schapery [14] on the basis of Hill's limitation for the effective mechanical properties of composites [2]. For modulus, the relationship for E_{11} is

$$E_{11} = E_m(1-\phi) + E_f\phi \tag{27}$$

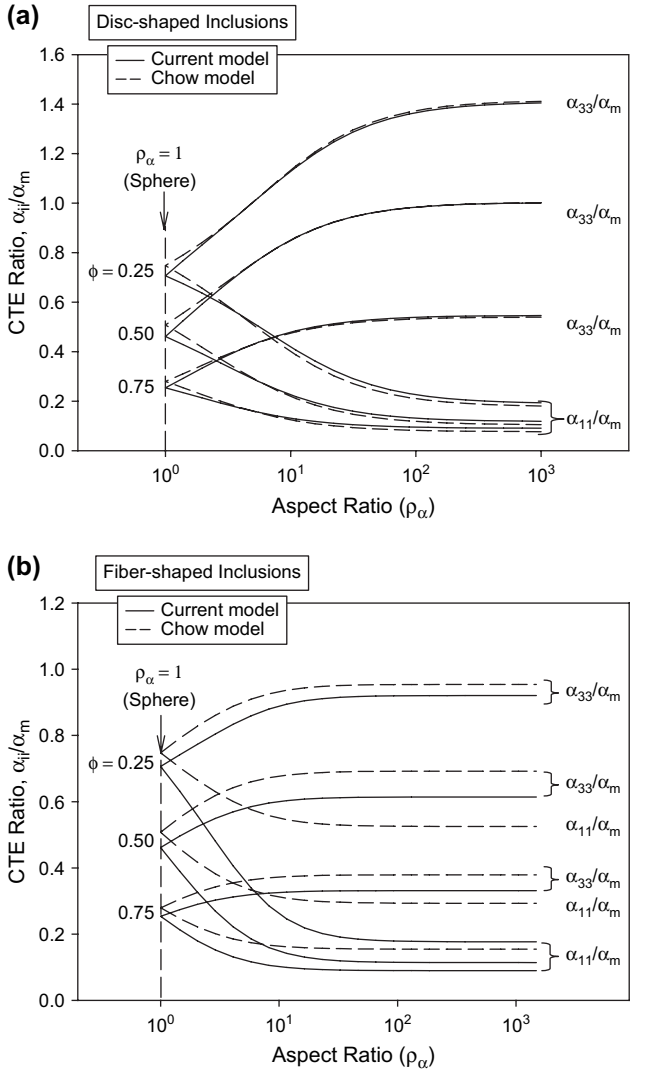

Fig. 3. Comparison of normalized coefficients of longitudinal, α_{11}/α_m, and transverse, α_{33}/α_m, thermal expansion for the disc-shaped (a) and fiber-shaped inclusions (b) computed for the current model and the Chow model as a function of the aspect ratio, $\rho_\alpha = a_1/a_3$, for fixed volume fractions of filler, $\phi = 0.25$, 0.5 and 0.75 where the components have the properties listed in Table 1.

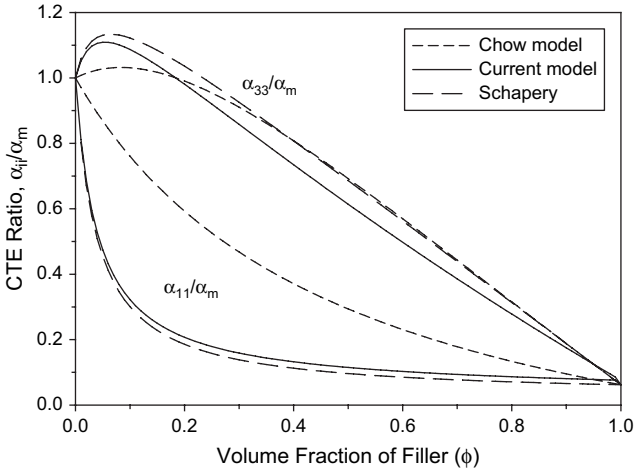

Fig. 4. Comparison of normalized coefficients of longitudinal, α_{11}/α_m, and transverse, α_{33}/α_m, thermal expansion for the fiber-shaped inclusions as a function of the volume fraction of filler, ϕ, for fixed aspect ratios, $\rho_\alpha = 100$ for the Chow model and the current model and $\rho_\alpha \to \infty$ for Schapery's theory.

This result is actually valid for an arbitrary number of fibers regardless of the Poisson's ratio, since the fibers and matrix do not interact under loading in the x_i-direction. Thus, the axial coefficient can be expressed in terms of the Young's modulus of each phase. The relationship for the longitudinal CTE, α_{11}, given by Schapery [14] is

$$\alpha_{11} = \frac{E_m\alpha_m(1-\phi) + E_f\alpha_f\phi}{E_m(1-\phi) + E_f\phi} \tag{28}$$

For the prediction of the transverse CTE, the transverse tensile moduli approach values close to the lower bound in the limit as $\rho_\alpha \to \infty$; hence, the mean values for α_{22} and α_{33} will be close to the rule-of-mixtures. The relationship for the transverse CTE, α_{33}, given by Schapery is

$$\alpha_{33} = (1+\nu_m)\alpha_m(1-\phi) + (1+\nu_f)\alpha_f\phi - \alpha_{11}(\alpha_m(1-\phi) + \nu_f\phi) \tag{29}$$

Predicted longitudinal, α_{11}/α_m, and transverse, α_{33}/α_m, CTE ratios versus the volume fraction of filler, ϕ, for fiber-shaped inclusions are compared in Fig. 4 for fixed aspect ratios, $\rho_\alpha = 100$ for the Chow model and the current model and $\rho_\alpha \to \infty$ for Schapery's theory. The limiting values of α_{11}/α_m from Schapery's theory are the lowest, because the composite is assumed to consist of a matrix with relatively stiff and parallel fibers that are continuous and unidirectionally aligned. The current model gives a result just slightly greater than Schapery's limit. Whereas the Chow model gives very different results for α_{11}/α_m. The current model gives lower values of α_{33}/α_m than Schapery's theory but the trends are similar; at high volume fractions, the Chow model matches the values from Schapery's theory quite well. In Table 2, normalized longitudinal, transverse, and bulk, CTEs are compared for the fiber-shaped inclusions for fixed aspect ratios, $\rho_\alpha = 100$ with the Chow model and the current model and $\rho_\alpha \to \infty$ with Schapery's theory.

Fig. 5 shows the normalized coefficients of longitudinal, α_{11}/α_m, transverse, α_{33}/α_m, and bulk thermal expansion, $\gamma/3\alpha_m$, as a function of volume fraction of filler for aspect ratios $\rho_\alpha = 10$ (Fig. 5(a)) and 100 (Fig. 5(b)) for disc and fiber-shaped inclusions. As the volume fraction of filler ϕ increases, α_{11} monotonically decreases for all aspect ratios and shapes owing to the mechanical constraint effect. On the contrary, α_{33} first increases owing to the compensation for the decrease in α_{11} but then decreases and eventually becomes less than α_m at high loadings owing to the dilution effect. For fibers, the normalized longitudinal coefficients, α_{11}/α_m, decrease faster than that for discs for both aspect ratios considered. On the contrary, the transverse coefficients, α_{33}/α_m, for the discs are larger than for the fibers for both aspect ratios. However, the effect of particle shape on the normalized bulk CTE $\gamma/3\alpha_m$ is relatively small compared with both of the linear CTE. The values for discs are slightly smaller than those for fibers.

The maximum in α_{33} versus ϕ means that for a given aspect ratio different loadings, i.e., values of ϕ, can exhibit the same value of α_{33}. Because of the conflicting effects that determine the predicted values of α_{33}, plots of α_{33}/α_m versus aspect ratio for one value of ϕ may cross a line for another value of ϕ once or even twice as illustrated in Fig. 6.

The range of volume fractions where $\alpha_{33} > \alpha_m$ is much broader for composites containing disc-shaped inclusions than those containing fibers; likewise the extent to which α_{33} exceeds α_m in this region is considerably greater for discs than fibers. The lines in Fig. 7 define the locus of ϕ and ρ_α values where $\alpha_{33} = \alpha_m$ (other than $\phi = 0$) for discs and for fibers. The regions where $\alpha_{33} > \alpha_m$ lie above and to the left of each curve. This condition occurs at lower aspect ratios and over a broader range of ϕ for discs than fibers. This stems from the fact the discs can constrain matrix expansion in two directions while fibers can do so in only one; this means that

Table 2
Comparison of normalized coefficients of longitudinal, α_{11}/α_m, transverse, α_{33}/α_m, and bulk, $\gamma/3\alpha_m$, thermal expansion for the fiber-shaped inclusions for fixed aspect ratios, $\rho_\alpha = 100$ with the Chow model and the current model and $\rho_\alpha \to \infty$ with Schapery's theory

Volume fraction of filler	Chow model			Schapery's theory			Current model		
	α_{11}/α_m	α_{33}/α_m	$\gamma/3\alpha_m$	α_{11}/α_m	α_{33}/α_m	$\gamma/3\alpha_m$	α_{11}/α_m	α_{33}/α_m	$\gamma/3\alpha_m$
25%	0.525	0.954	0.811	0.158	0.982	0.707	0.179	0.920	0.673
50%	0.294	0.692	0.559	0.0961	0.686	0.489	0.115	0.614	0.448
75%	0.155	0.379	0.304	0.073	0.376	0.275	0.090	0.331	0.251

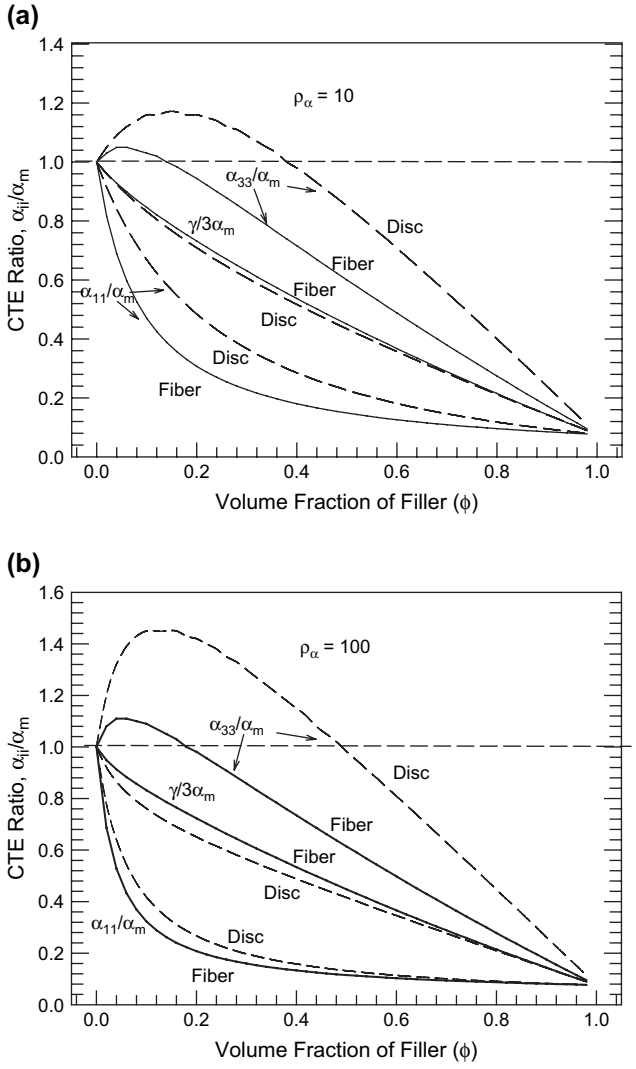

Fig. 5. Normalized coefficients of longitudinal, α_{11}/α_m, transverse, α_{33}/α_m, and bulk, $\gamma/3\alpha_m$, thermal expansion for disc-shaped (closed) and fiber-shaped (open) inclusions as a function of filler volume fraction for aspect ratios $\rho_\alpha =$ 10 (a) and 100 (b).

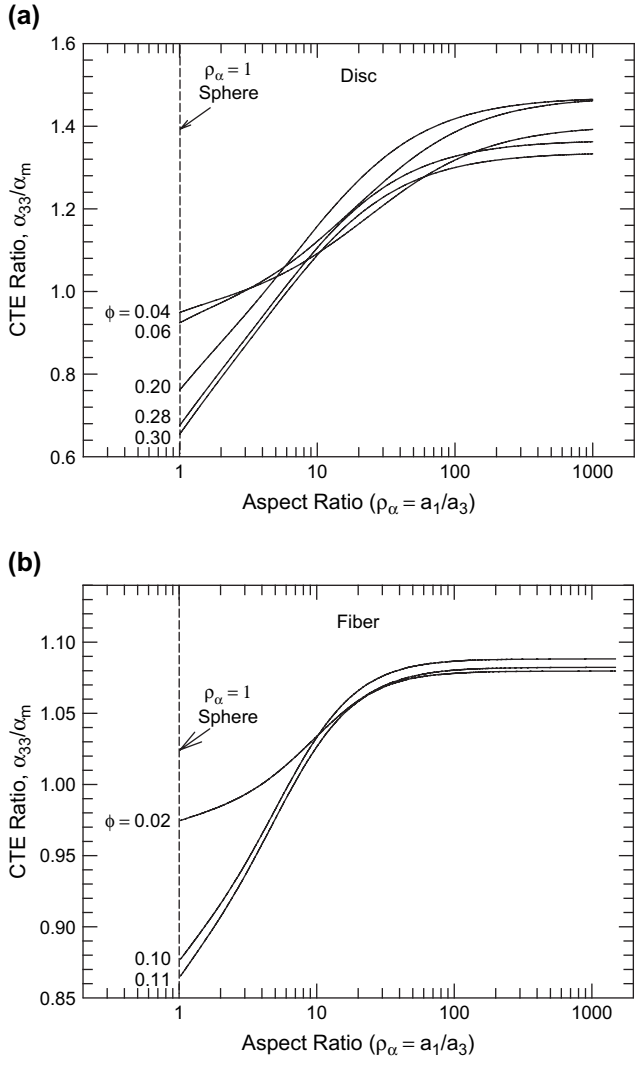

Fig. 6. Normalized coefficients of transverse thermal expansion, α_{33}/α_m, as a function of aspect ratio ρ_α for volume fractions ϕ selected to illustrate how the non-monotonic relation with ϕ affect the trend with ρ_α, for disc-shaped (a) and the fiber-shaped inclusions (b).

the squeezing effect that causes $\alpha_{33} > \alpha_m$ is greater in magnitude and over a broader region of ϕ for discs than fibers.

Fig. 8 shows the normalized bulk CTE (the sum of the longitudinal and the transverse CTEs) normalized by that of the isotropic matrix, i.e., $\gamma/3\alpha_m$, as a function of the aspect ratio for fixed volume fractions of filler. For the numerical case being considered, the bulk thermal expansion decreases, as ρ_α and ϕ increase. Since the longitudinal and the transverse CTEs can show opposite trends, there is a tendency for cancellation of the effects of mechanical constraint by the inclusions. Hence, the bulk CTE shows much less effect of the aspect ratio of the filler than do the linear CTE. The bulk CTE of composites more nearly complies with a linear mixture rule; however, the values calculated from the current model are a little less than this for spheres, $\rho_\alpha = 1$, and decrease to a certain lower-limit value, as the aspect ratios increase. The extent of the decrease is greater for discs than fibers, as seen in

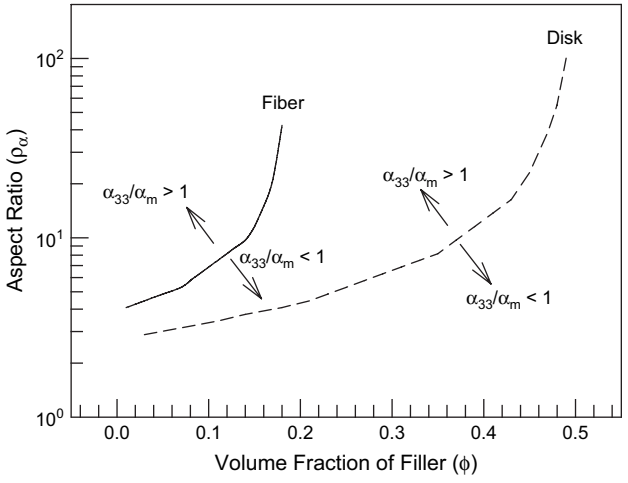

Fig. 7. Regions of filler volume fraction and aspect ratio where the normalized coefficient of transverse thermal expansion, α_{33}/α_m, is greater than or less than unity for fiber-shaped (closed) and disc-shaped (open) inclusions.

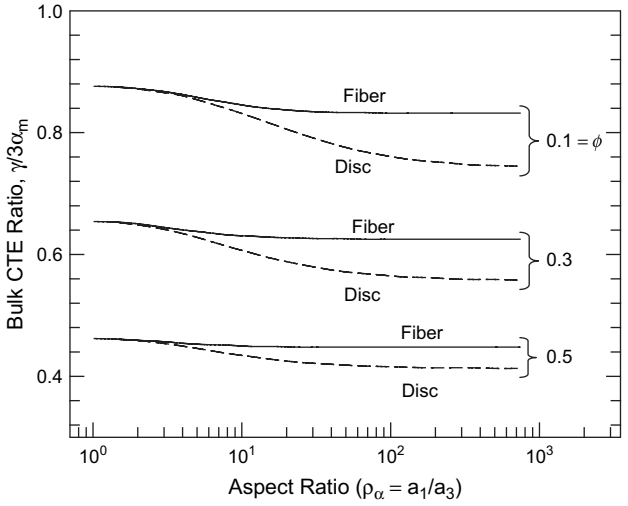

Fig. 8. Comparison of normalized bulk coefficients of thermal expansion, $\gamma/3\alpha_m$, for disc-shaped and fiber-shaped inclusions as a function of aspect ratio, ρ_α, for fixed filler volume fractions.

Fig. 8, owing to the two-dimensional versus one-dimensional constraints inherent to these shapes.

5. Conclusion

The model described here differs in some details from the Chow model [10–12] and is believed to be more accurate; an important advantage of the current approach is that it provides a useful route to develop a model for inclusions having more complex shapes, described by two aspect ratios, as presented in a subsequent paper.

Calculations are presented here for filler particles that have a higher modulus and lower CTE (glass particles) than the matrix (an epoxy resin). For $\rho_\alpha = 1$ (spheres), the thermal coefficients decrease as ϕ increases due to the dilution of the high CTE matrix with a low CTE filler. As the aspect ratio increases, the linear coefficient of thermal expansion in the direction of filler alignment, α_{11}, decreases for all ϕ due to the mechanical constraint the filler provides against the expansion of the matrix. On the other hand, the expansion in the perpendicular direction, α_{33}, increases with aspect ratio for certain values of ϕ, since the restraint squeezes the polymer matrix out in this direction. The reduction in α_{11} is greater for fibers than discs while the increase in α_{33} is greater for discs than fibers. These differences stem from the two-dimensional constraints caused by discs ($\alpha_{11} = \alpha_{22} < \alpha_{33}$) versus the one-dimensional effect of fibers ($\alpha_{11} < \alpha_{22} = \alpha_{33}$). The opposite thermal expansion behavior in the longitudinal and transverse directions leads to a much smaller effect on the volumetric expansion caused by inclusions. The values of α_{11}, α_{33} and γ approach limiting values for each ϕ, for either shape, as the aspect ratio becomes large (over 100). Such plateau values approximate the properties of composites, comprised of very long fibers (or platelets). The values of α_{11}/α_m monotonically decrease for both discs and fibers, as the filler volume fraction increases for a given aspect ratio, while the values of α_{33}/α_m initially increase, go through maxima and eventually become less than unity. There exist crossover points at certain conditions for α_{33}/α_m as a function of aspect ratio at a given filler volume fraction.

Acknowledgment

This study was financially supported by research funds provided by Chungnam National University in 2006.

Appendix

The following components of Eshelby's S_{ijkl} tensor for the cases that approximate spheres, discs and fibers are given below.

For spherical inclusions ($a_1 = a_2 = a_3$ or $\rho_\alpha = 1$)

$$S_{1111} = S_{2222} = S_{3333} = \frac{7 - 5\nu_m}{15(1 - \nu_m)}$$

$$S_{1122} = S_{2233} = S_{3311} = \frac{5\nu_m - 1}{15(1 - \nu_m)}$$

$$S_{1212} = S_{2323} = S_{3131} = \frac{4 - 5\nu_m}{15(1 - \nu_m)}$$

For disc-shaped inclusions ($a_1 = a_2 > a_3$)

$$S_{1111} = \frac{1}{2(1-\nu_m)}\left\{1 - 2\nu_m + \frac{\rho_\alpha^2 - 3}{\rho_\alpha^2 - 1} - \left[1 - 2\nu_m - \frac{3}{\rho_\alpha^2 - 1}\right] G_d(\rho_\alpha)\right\}$$

$$S_{2222} = S_{3333} = -\frac{3}{8(1-\nu_m)}\frac{1}{\rho_\alpha^2 - 1} + \frac{1}{4(1-\nu_m)} \times \left[1 - 2\nu_m + \frac{9\rho_\alpha^2}{4(\rho_\alpha^2 - 1)}\right] G_d(\rho_\alpha)$$

$$S_{2233} = S_{3322} = -\frac{1}{4(1-\nu_m)}\left\{\frac{1}{2(\rho_\alpha^2 - 1)} + \left[1 - 2\nu_m - \frac{3\rho_\alpha^2}{4(\rho_\alpha^2 - 1)}\right] G_d(\rho_\alpha)\right\}$$

$$S_{2211} = S_{3311} = \frac{1}{2(1-\nu_m)}\frac{1}{\rho_\alpha^2 - 1} - \frac{1}{4(1-\nu_m)}\left\{\frac{3}{\rho_\alpha^2 - 1} + (1 - 2\nu_m)\right\} G_d(\rho_\alpha)$$

$$S_{1122} = S_{1133} = -\frac{1}{2(1-\nu_m)}\left[1-2\nu_m-\frac{\rho_\alpha^2}{\rho_\alpha^2-1}\right] + \frac{1}{2(1-\nu_m)}\left[1-2\nu_m-\frac{3\rho_\alpha^2}{2(\rho_\alpha^2-1)}\right]G_d(\rho_\alpha)$$

$$S_{2323} = S_{3232} = -\frac{1}{4(1-\nu_m)}\left\{\frac{1}{2(\rho_\alpha^2-1)} - \left[1-2\nu_m + \frac{3\rho_\alpha^2}{4(\rho_\alpha^2-1)}\right]G_d(\rho_\alpha)\right\}$$

$$S_{1212} = S_{1313} = \frac{1}{4(1-\nu_m)}\left\{1-2\nu_m+\frac{\rho_\alpha^2+1}{\rho_\alpha^2-1} - \frac{1}{2}\left[1-2\nu_m + \frac{3(\rho_\alpha^2+1)}{\rho_\alpha^2-1}\right]G_d(\rho_\alpha)\right\}$$

where ν_m and ρ_α are Poisson's ratio of the matrix and the aspect ratio of the inclusion ($\rho_\alpha = a_1/a_3$), respectively, and $G_d(\rho_\alpha)$ is given by

$$G_d(\rho_\alpha) = \frac{1}{(\rho_\alpha^2-1)^{3/2}}\left\{\rho_\alpha^2\ \cosh^{-1}\left(\frac{1}{\rho_\alpha}\right) - (\rho_\alpha^2-1)^{1/2}\right\}$$

For fiber-shaped inclusions

$$S_{1111} = \frac{1}{2(1-\nu_m)}\left\{1-2\nu_m+\frac{3\rho_\alpha^2-1}{\rho_\alpha^2-1} - \left[1-2\nu_m+\frac{3\rho_\alpha^2}{\rho_\alpha^2-1}\right]G_f(\rho_\alpha)\right\}$$

$$S_{2222} = S_{3333} = \frac{3}{8(1-\nu_m)}\frac{\rho_\alpha^2}{\rho_\alpha^2-1} + \frac{1}{4(1-\nu_m)}\left[1-2\nu_m - \frac{9}{4(\rho_\alpha^2-1)}\right]G_f(\rho_\alpha)$$

$$S_{2233} = S_{3322} = \frac{1}{4(1-\nu_m)}\left\{\frac{\rho_\alpha^2}{2(\rho_\alpha^2-1)} - \left[1-2\nu_m+\frac{3}{4(\rho_\alpha^2-1)}\right]G_f(\rho_\alpha)\right\}$$

$$S_{2211} = S_{3311} = -\frac{1}{2(1-\nu_m)}\frac{\rho_\alpha^2}{\rho_\alpha^2-1} + \frac{1}{4(1-\nu_m)}\left\{\frac{3\rho_\alpha^2}{\rho_\alpha^2-1} - (1-2\nu_m)\right\}G_f(\rho_\alpha)$$

$$S_{1122} = S_{1133} = -\frac{1}{2(1-\nu_m)}\left[1-2\nu_m+\frac{1}{\rho_\alpha^2-1}\right] + \frac{1}{2(1-\nu_m)}\left[1-2\nu_m + \frac{3}{2(\rho_\alpha^2-1)}\right]G_f(\rho_\alpha)$$

$$S_{2323} = S_{3232} = \frac{1}{4(1-\nu_m)}\left\{\frac{\rho_\alpha^2}{2(\rho_\alpha^2-1)} + \left[1-2\nu_m-\frac{3}{4(\rho_\alpha^2-1)}\right]G_f(\rho_\alpha)\right\}$$

$$S_{1212} = S_{1313} = \frac{1}{4(1-\nu_m)}\left\{1-2\nu_m-\frac{\rho_\alpha^2+1}{\rho_\alpha^2-1} - \frac{1}{2}\left[1-2\nu_m - \frac{3(\rho_\alpha^2+1)}{\rho_\alpha^2-1}\right]G_f(\rho_\alpha)\right\}$$

where $G_f(\rho_\alpha)$ is given by

$$G_f(\rho_\alpha) = \frac{\rho_\alpha}{(\rho_\alpha^2-1)^{3/2}}\left\{\rho_\alpha(\rho_\alpha^2-1)^{1/2} - \cosh^{-1}\ \rho_\alpha\right\}$$

References

[1] Eshelby JD. Proc R Soc London 1957;A241(1226):376–96.
[2] Hill R. J Mech Phys Solids 1964;12:199–212.
[3] Mori T, Tanaka K. Acta Metall 1963;21:571–4.
[4] Halpin JC. Technical report 67-423. Air Force Materials Laboratory; 1969.
[5] Tandon GP, Weng GJ. Polym Compos 1984;5:327–33.
[6] Mura T. Micromechanics of defects in solids. 2nd ed. The Hague: Martinus Nijhoff; 1987. p. 74.
[7] Tucker CL, Liang E. Compos Sci Technol 1999;59:655–71.
[8] Yoon PJ, Fornes TD, Paul DR. Polymer 2002;43(25):6727–41.
[9] Lee KY, Paul DR. Polymer 2005;46(21):9064–80.
[10] Chow TS. J Polym Sci Polym Phys Ed 1978;16:959–65.
[11] Chow TS. J Polym Sci Polym Phys Ed 1978;16:967–70.
[12] Chow TS. J Mater Sci 1980;15:1873–88.
[13] Takao Y, Taya M. Trans ASME 1985;52:806–10.
[14] Schapery RA. J Compos Mater 1968;2:380–404.
[15] Wakashima K, Otsuka M, Umekawa S. J Compos Mater 1974;8:391–404.
[16] Holliday L, Robinson J. J Mater Sci 1973;8:301–11.
[17] Segal L. Polym Eng Sci 1979;19:365–72.
[18] Feltham SJ, Yates B, Martin RJ. J Mater Sci 1982;17:2309–23.
[19] Ahmed S, Jones FR. J Mater Sci 1990;25:4933–42.
[20] Bozec YL, Kaang S, Hine PJ, Ward IM. Compos Sci Technol 2000;60:333–44.
[21] Ellis TS, D'Angelo JS. J Appl Polym Sci 2003;90:1639–47.
[22] Wei C, Srivastava D, Cho K. Nano Lett 2002;2(6):647–50.
[23] Lee HS, Fasulo PD, Rodgers WR, Paul DR. Polymer 2005;46(25):11673–89.
[24] Lee HS, Fasulo PD, Rodgers WR, Paul DR. Polymer 2006;47(10):3528–39.
[25] Bowles DE, Tompkins SS. J Compos Mater 1989;23:370–88.
[26] Pierard O, Friebel C, Doghri I. Compos Sci Technol 2004;64:1587–603.

[27] Li JU. Mech Mater 1999;31:149–59.
[28] Doghri I, Tinel L. Comput Methods Appl Mech Eng 2006;195: 1387–406.
[29] Lusti HR, Hine PJ, Gusev AA. Compos Sci Technol 2002;62: 1927–34.
[30] Dray D, Gilormini P, Regnier G. Compos Sci Technol 2007;67(7–8): 1601–10.
[31] Hbaieb K, Wang QX, Chia YHJ, Cotterrell B. Polymer 2007;48:901–9.
[32] Lee SM. International encyclopedia of composites. New York: VCH Pub Inc; 1990.